Chapter 1

Understanding Diffraction in Volume Gratings and Holograms

Brotherton-Ratcliffe David

Additional information is available at the end of the chapter

http://dx.doi.org/10.5772/53413

1. Introduction

Kogelnik's Coupled wave theory [1], published in 1969, has provided an extremely successful approach to understanding diffraction in sinusoidal volume gratings and in providing analytic formulae for the calculation of diffractive efficiency. N-coupled wave theory [2] has extended Kogelnik's approach to provide a useful analytic model of diffraction in spatially multiplexed gratings and in monochromatic holograms.

A more recent and alternative approach to Kogelnik's coupled wave theory, known as the PSM model [3], short for "Parallel Stacked Mirrors", is based on a differential formulation of the process of Fresnel reflection occurring within the grating. This theory has the advantage of providing a particularly useful and more intuitively natural description of diffraction in the reflection volume grating. It also deals with the π-polarisation, which requires significantly greater work under Kogelnik's approach, in a simpler and more natural way.

Although the PSM model is itself a type of coupled-wave theory, it is nevertheless based on an alternative and distinct set of assumptions to standard coupled-wave theory. This in itself is extremely useful as it allows one to look at the problem of diffraction in volume gratings from two relatively separate perspectives. In some cases the PSM assumptions are clearly somewhat superior to Kogelnik's as evidenced by rigorous computational solutions of the Helmholtz equation. But this is not always the case and in various albeit rather extreme cases Kogelnik's theory can provide the superior estimate of diffractive efficiency.

The PSM model naturally treats polychromatic index modulation profiles. This is not to say that Kogelnik's formulism cannot be extended to treat the polychromatic case. Indeed Ning has demonstrated this [4]. But the mathematics and their meaning here is more transparent in the PSM case. Like standard coupled-wave theory, the PSM model can be generalised to an N-coupled wave theory, capable of describing spatially multiplexed gratings and holograms. Again the PSM model provides a simple and trivially transparent generalisation to the polychromatic spatially multiplexed grating allowing a very clear understanding of diffraction in the full-colour reflection volume hologram.

Despite the utility and analytic nature of both Kogelnik's coupled wave theory and the PSM model, a completely accurate description of diffraction in gratings can only be offered by a rigorous solution of the underlying wave equation. Moharam and Gaylord [5] first tackled this problem in 1989 and provided numerical solutions for both transmission and reflection gratings as index modulation increased. Glytis and Gaylord [6] extended this work to cover anistropic media and simple multiplexed gratings.

2. Kogelnik's coupled wave theory

Kogelnik's theory [1] assumes that only two plane waves propagate inside and outside a finite thickness grating. The Helmholtz equation is then used to calculate how a specific modulation in the dielectric permittivity intrinsically couples these waves. The approach has its origins in the field of acousto-optics. The first wave is assumed to be the illuminating reference wave and the second wave is the hologram's response or "signal" wave. The adoption of just two waves is made on the assumption that coupling to higher order modes will be negligible. There is no rigorous mathematical proof for this per se; we therefore look to the results of this two-wave theory to see whether they are sensible and consistent. In addition we shall review a rigorous formulation of the coupled wave equations in section 5 and here we shall see that for the kind of index modulations present in modern holography, the two-wave assumption is pretty good.

2.1. Derivation of the coupled wave equations

Assuming a time dependence of $\sim \exp(i\omega t)$ Maxwell's equations and Ohm's law can be used to write down the general wave equation for a dielectric in SI units:

$$\nabla \times (\nabla \times \boldsymbol{E}) - \gamma^2 \boldsymbol{E} = 0 \tag{1}$$

$$\text{where} \quad \gamma^2 = i\omega\mu\sigma - \omega^2 \mu\varepsilon \tag{2}$$

Here μ is the permeability of the medium, ε its permittivity and σ represents its electrical conductivity. Two important assumptions are now made. The first is that the grating is lossless so that $\sigma = 0$. The second is that the polarization of the two waves is perpendicular to the grating vector or $\boldsymbol{E} \cdot \nabla \varepsilon = 0$. This allows (1) to be simplified to the Helmholtz equation

$$\nabla^2 \boldsymbol{E} - \gamma^2 \boldsymbol{E} = 0 \tag{3}$$

The assumption of small conductivity means that our analysis is restricted to lossless phase holograms with no absorption. The assumption that $\boldsymbol{E}\cdot\nabla\varepsilon=0$ leads us to study the σ-polarisation.

2.1.1. One-dimensional grating

A one-dimensional grating extending from $x=0$ to $x=d$ is now assumed. The relative permittivity is also assumed to vary within the grating according to the following law:

$$\varepsilon_r=\varepsilon_{r0}+\varepsilon_{r1}\cos\boldsymbol{K}\cdot\boldsymbol{r} \tag{4}$$

The grating vector $\boldsymbol{K}$ is defined by its slope, ϕ and its pitch, Λ

$$\boldsymbol{K}=\frac{2\pi}{\Lambda}\begin{pmatrix}\cos\phi\\ \sin\phi\end{pmatrix} \tag{5}$$

We may write the γ parameter in (2) as

$$\gamma^2\sim-\beta^2-4\kappa\beta\cos\boldsymbol{K}\cdot\boldsymbol{r} \tag{6}$$

$$\text{with}\quad \beta=\omega(\mu\varepsilon_0\varepsilon_{r0})^{1/2} \tag{7}$$

Here we have also introduced Kogelnik's coupling constant

$$\kappa\equiv\frac{1}{4}\frac{\varepsilon_{r1}}{\varepsilon_{r0}}\beta\sim\frac{1}{2}(\frac{n_1}{n_0})\beta \tag{8}$$

2.1.2. Solution at Bragg resonance

At Bragg resonance the signal and reference wavevectors are related by the condition

$$\boldsymbol{k}_i=\boldsymbol{k}_c-\boldsymbol{K} \tag{9}$$

The magnitude of both $\boldsymbol{k}_c$, the reference wavevector, and of $\boldsymbol{k}_i$, the signal wavevector is also exactly $\beta=2\pi n/\lambda_c$. Accordingly (6) may be written as

$$\gamma^2=-\beta^2-4\kappa\beta\cos(\boldsymbol{k}_c-\boldsymbol{k}_i)\cdot\boldsymbol{r} \tag{10}$$

$$\text{with}\,\boldsymbol{k}_c=\beta\begin{pmatrix}\cos\theta_c\\ \sin\theta_c\end{pmatrix}\quad ;\quad \boldsymbol{k}_i=\beta\begin{pmatrix}\cos\theta_i\\ \sin\theta_i\end{pmatrix}=\beta\begin{pmatrix}\cos\theta_c\\ \sin\theta_c\end{pmatrix}-\frac{2\pi}{\Lambda}\begin{pmatrix}\cos\phi\\ \sin\phi\end{pmatrix}\tag{11}$$

We now choose a very particular trial solution of the form

$$E_z=R(x)e^{-i\boldsymbol{k}_c\cdot\boldsymbol{r}}+S(x)e^{-i\boldsymbol{k}_i\cdot\boldsymbol{r}}\tag{12}$$

The first term represents the illumination or "reference" wave and the second term, the response or "signal" wave. Both are plane waves. Figure 1(a) illustrates how these waves propagate in a reflection grating and Figure 1(b) illustrates the corresponding case of the transmission hologram. Note that the complex functions R and S are functions of x only - even though the wave-vectors $\boldsymbol{k}_c$ and $\boldsymbol{k}_i$ both possess x and y components. The grating is assumed to be surrounded by a dielectric having the same permittivity and permeability as the average values within the grating so as not to unduly complicate the problem with boundary reflections. Within the external dielectric both R and S are constants. The choice of just using two waves in the calculation - clearly the absolute minimum - and with only a one-dimensional behaviour was inspired by the work of Bhatia and Noble [7] and Phariseau [8] in the field of acousto-optics.

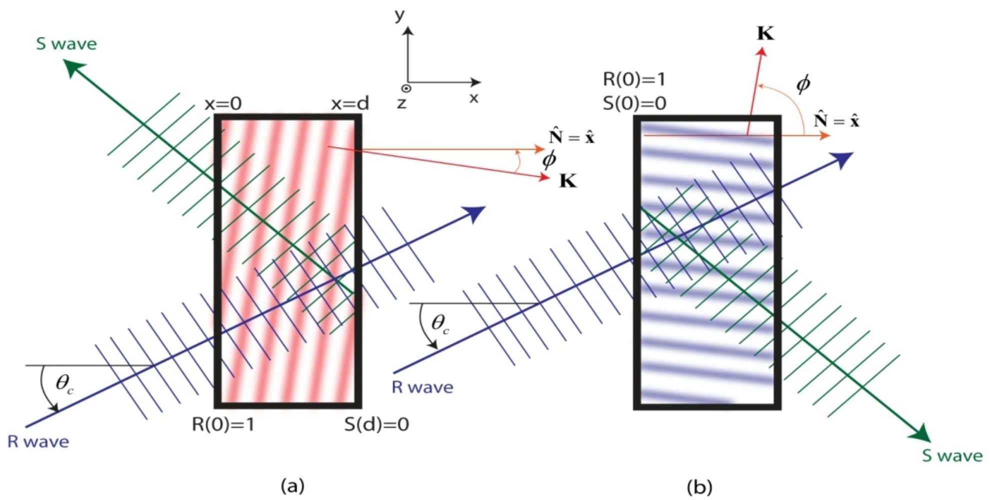

Figure 1. The "R" and "S" waves of Kogelnik's Coupled Wave Theory for the case of (a) a reflection grating and (b) a transmission grating.

Substituting (12) into (3) we obtain

$$e^{-i\boldsymbol{k}_c\cdot\boldsymbol{r}}\left\{\frac{d^2R}{dx^2}-2ik_{cx}\frac{dR}{dx}+2\beta\kappa S\right\}+e^{-i\boldsymbol{k}_i\cdot\boldsymbol{r}}\left\{\frac{d^2S}{dx^2}-2ik_{ix}\frac{dS}{dx}+2\beta\kappa R\right\}$$
$$+2\beta\kappa S e^{-i(2\boldsymbol{k}_i-\boldsymbol{k}_c)\cdot\boldsymbol{r}}+2\beta\kappa R e^{-i(2\boldsymbol{k}_c-\boldsymbol{k}_i)\cdot\boldsymbol{r}}=0 \tag{13}$$

Since only two waves are assumed to exist in the solution we must now disregard the third and fourth term of this expression on the pretext that they inherit only negligible energy from the primary modes. Next, second-order derivatives are neglected on the premise that R and S are slowly varying functions. Then (13) reduces to the two coupled first-order ordinary differential equations:

$$\frac{k_{cx}}{\beta}\frac{dR}{dx}+i\kappa S=0 \tag{14}$$

$$\frac{k_{ix}}{\beta}\frac{dS}{dx}+i\kappa R=0 \tag{15}$$

We can then use (14) and (15) to derive identical uncoupled second order differential equations for R and S:

$$\frac{d^2R}{dx^2}+(\kappa^2\sec\theta_c\sec\theta_i)R=0;\ \frac{d^2S}{dx^2}+(\kappa^2\sec\theta_c\sec\theta_i)S=0 \tag{16}$$

Here the x component of the Bragg condition tells us that

$$\sec\theta_i=\left\{\cos\theta_c-\frac{\lambda_c K_x}{2\pi n_0}\right\}^{-1} \tag{17}$$

And if the grating has been written using a reference and object wave of angles of incidence of respectively θ_r and θ_o and at a wavelength of λ_r then

$$K_x=\frac{2\pi n_0}{\lambda_r}(\cos\theta_r-\cos\theta_o) \tag{18}$$

2.1.3. Boundary conditions

It has been assumed that the R wave is the driving wave and that the S wave is the response or "signal" wave. Clearly, and without loss of generality, the input amplitude of the driving wave can be normalised to unity. Then different boundary conditions can be written down for transmission and reflection gratings. For transmission gratings the choice of normalisation means that $R(0)=1$. In addition we demand that $S(0)=0$ as the power of the transmitted signal wave must be zero at the input boundary as evidently no conversion has yet taken place at this point. For reflection holograms we demand once again that $R(0)=1$ but now the second boundary condition is $S(d)=0$. This is because the reflected response wave travels in the direction $x=d$ to $x=0$ and its amplitude must clearly be zero at the far boundary.

With these boundary conditions in hand we can now solve (14) - (15) for the transmission and reflection cases. For the transmission grating we obtain

$$\begin{aligned} R &= \cos\{\kappa x(\sec\theta_c \sec\theta_i)^{1/2}\} \\ S &= -i\sqrt{\frac{\cos\theta_c}{\cos\theta_i}}\sin\{\kappa x(\sec\theta_c \sec\theta_i)^{1/2}\} \end{aligned} \tag{19}$$

And for the reflection grating we have

$$\begin{aligned} R &= \operatorname{sech}\{\kappa d(\sec\theta_c \mid \sec\theta_i \mid)^{1/2}\}\cosh\{\kappa(d-x)(\sec\theta_c \mid \sec\theta_i \mid)^{1/2}\} \\ S &= -i\sqrt{\frac{\cos\theta_c}{\mid\cos\theta_i\mid}}\operatorname{sech}\{\kappa d(\sec\theta_c \mid \sec\theta_i \mid)^{1/2}\}\sinh\{\kappa(d-x)(\sec\theta_c \mid \sec\theta_i \mid)^{1/2}\} \end{aligned} \tag{20}$$

These are very simple solutions which paint a rather logical picture. For the transmission case we see that as the reference wave enters the grating it slowly donates power to the signal wave which grows with increasing x. When the argument of the cosine function in (19) reaches $\pi/2$ all of the power has been transferred to the S wave which is now at a maximum. As x increases further the waves change roles; the S wave now slowly donates power to a newly growing R wave. This process goes on until the waves exit the grating at $x=d$.

In the reflection case the behaviour is rather different. Here, as one might well expect, there is simply a slow transfer of energy from the reference driving wave to the reflected signal wave. If the emulsion is thin then the signal wave is weak and most of the energy escapes as a transmitted R wave. If the emulsion is thick on the other hand then the amplitudes of both waves become exponentially small as x increases and all the energy is transferred from the R wave to the reflected S wave.

2.1.4. Power balance and diffraction efficiency

Using Poynting's theorem it can be shown that power flowing along the x direction is given by

$$P = \cos\theta_c RR^* + \cos\theta_i SS^* \tag{21}$$

Multiplying (21) by respectively R^* and S^* and then adding these equations and taking the real part results in the equation

$$\frac{dP}{dx} = 0 \tag{22}$$

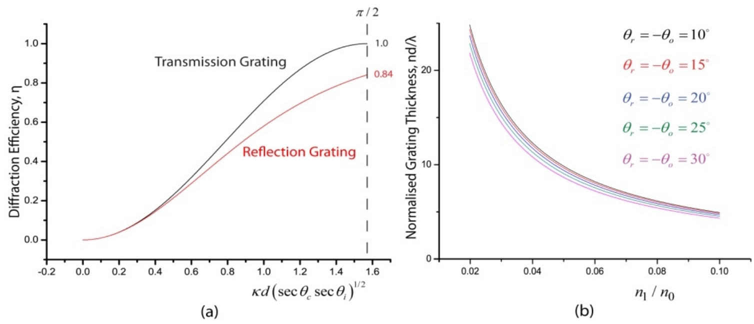

Figure 2. Perfect Bragg Compliance: (a) Diffractive replay efficiencies (σ-polarisation) of the transmission grating and the reflection grating versus the normalised grating thickness according to Kogelnik's coupled wave theory. (b) Optimal value of the normalised grating thickness (providing $\eta_T = 1$) at Bragg Resonance versus the modulation, n_1 / n_0 for the unslanted transmission grating recorded at various (internal) angles, $\theta_r = -\theta_o$.

This tells us that at each value of x the power in the R wave and in the S wave change but that the power in both waves taken together remains a constant. Now it is of particular interest to understand the efficiency of a holographic grating. With this in mind we define the diffraction efficiency of a grating illuminated by a reference wave of unit amplitude as

$$\eta = \frac{|\cos\theta_i|}{\cos\theta_c} S S^* \tag{23}$$

where S is evaluated on the exit boundary which for a reflection hologram will be at $x = 0$ and for a transmission hologram at $x = d$.

It is now simple to use the forms for R and S given in (19) and (20) to calculate the expected diffractive efficiencies for the transmission and reflection grating:

$$\eta_T = \sin^2\{\kappa d(\sec\theta_c \sec\theta_i)^{1/2}\} \tag{24}$$

$$\eta_R = \tanh^2\{\kappa d(\sec\theta_c |\sec\theta_i|)^{1/2}\} \tag{25}$$

Figure 2(a) shows this graphically for $0 \le \kappa d(\sec\theta_c |\sec\theta_i|)^{1/2} \le \pi/2$. Clearly for a small emulsion thickness or for a small permittivity modulation, the diffractive efficiencies of the reflection and transmission types of hologram are identical. As the parameter $\kappa d(\sec\theta_c \sec\theta_i)^{1/2}$ increases towards $\pi/2$ the transmission hologram becomes slightly more diffractive than its corresponding reflection counterpart. However, as we have remarked above, when $\kappa d(\sec\theta_c \sec\theta_i)^{1/2} > \pi/2$, the transmission hologram decreases in diffractive response whereas the corresponding reflection hologram continues to produce an increasing response. Figure 2(b) shows the relationship between the optimum grating thickness at which the diffractive response of the (un-slanted) transmission grating peaks and the grating modulation, n_1 / n_0.

2.1.5. Behaviour away from Bragg resonance

To study the case of a small departure from the Bragg condition Kogelnik continues to use (9) but relaxes the condition that $|\boldsymbol{k}_i| = \beta$. This choice, which is certainly not unique, has the effect that the phases of the contributions of the signal wave from each Bragg plane no longer add up coherently and leads naturally to the definition of an "off-Bragg" parameter; this allows us in turn to easily quantify how much the Bragg condition is violated either in terms of wavelength or in terms of angle. Proceeding in this fashion, equation (14) remains the same but equation (15) generalizes to

$$\frac{k_{ix}}{\beta}\frac{dS}{dx} + i\left(\frac{\beta^2 - |k_i|^2}{2\beta}\right)S + i\kappa R = 0 \tag{26}$$

We then define the "Off-Bragg" or "dephasing" parameter

$$\vartheta = \frac{\beta^2 - |k_i|^2}{2\beta} = |\boldsymbol{K}|\cos(\phi - \theta_c) - \frac{|\boldsymbol{K}|^2}{2\beta} \tag{27}$$

where ϕ represents the slant angle between the grating normal and the grating vector (see Figure 1). The value of ϑ is determined by the angle of incidence on reconstruction (θ_c) and by the free-space wavelength of the illuminating light ($\lambda_c = 2\pi n_0 / \beta$). Clearly when $\vartheta = 0$ the Bragg condition is satisfied and $|\boldsymbol{k}_i| = \beta$. We define the obliquity factors

$$\begin{aligned} k_{ix}/\beta &= (|k_{ix}|/\beta)\cos\theta_i \equiv c_S \\ k_{cx}/\beta &= \cos\theta_c \equiv c_R \end{aligned} \tag{28}$$

Then, as before, we can solve equations (14) and (26) to arrive at expressions for the diffractive efficiency[1]. For the transmission grating the result is

$$\eta_T = \frac{\sin^2\left(\frac{\kappa^2 d^2}{c_R c_S} + \frac{d^2\vartheta^2}{4{c_S}^2}\right)^{1/2}}{1 + \frac{\vartheta^2 c_R}{4 c_S \kappa^2}} \tag{29}$$

1 Note that equation 23 is modified away from Bragg resonance in Kogelnik's theory to the more general form $\eta = \frac{|c_S|}{c_R} S S^*$

whereas for the reflection grating we have

$$\eta_R = \left\{ 1 + \frac{1 - \dfrac{\vartheta^2 c_R}{4|c_S|\kappa^2}}{\sinh^2\left(\dfrac{\kappa^2 d^2}{c_R|c_S|} - \dfrac{d^2\vartheta^2}{4c_S{}^2}\right)^{1/2}} \right\}^{-1} \tag{30}$$

Clearly for $\vartheta = 0$ these equations revert respectively to (24) and (25). Figures 3 (a) and (b) show the behaviour of (29) and (30) for several values of $\kappa d / (c_R \mid c_S \mid)^{1/2}$.

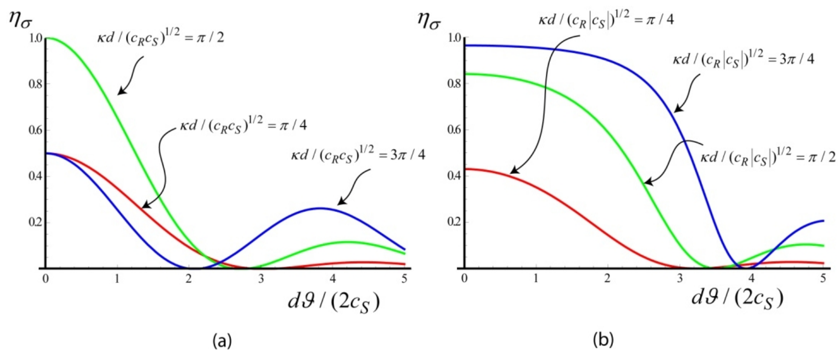

Figure 3. (a) Diffraction Efficiency for the transmission grating according to Kogelnik's theory versus the normalised Off-Bragg Parameter, $d / (2c_S)$ for different values of $\kappa d / (c_R c_S)^{1/2}$. (b) Corresponding graph for the reflection grating.

We can understand better the parameter ϑ if we imagine having recorded the grating, which we are now seeking to play back, with an object beam at angle of incidence θ_o and with a reference beam at angle θ_r. The recording wavelength is λ_r and we assume that there is no emulsion shrinkage and no change in average emulsion index on recording the grating. Then the various wave-vectors can be written as

$$\boldsymbol{k}_r = \frac{2\pi n}{\lambda_r}\begin{pmatrix}\cos\theta_r \\ \sin\theta_r\end{pmatrix}; \boldsymbol{k}_o = \frac{2\pi n}{\lambda_r}\begin{pmatrix}\cos\theta_o \\ \sin\theta_o\end{pmatrix} \tag{31}$$

$$\boldsymbol{k}_c = \frac{2\pi n}{\lambda_c}\begin{pmatrix}\cos\theta_c \\ \sin\theta_c\end{pmatrix}; \boldsymbol{k}_i = \mid k_i \mid \begin{pmatrix}\cos\theta_i \\ \sin\theta_i\end{pmatrix} \tag{32}$$

Then (27) can be written as

$$\vartheta = \frac{2\pi n}{\lambda_r}\{\cos(\theta_r - \theta_c) - \cos(\theta_o - \theta_c)\} - \frac{2\pi n \lambda_c}{\lambda_r{}^2}\{1 - \cos(\theta_r - \theta_o)\} \tag{33}$$

This tells us how the parameter ϑ behaves when $\lambda_c \neq \lambda_r$ and when $\theta_c \neq \theta_r$. Direct substitution of (33) into (29) and (30) leads trivially to general expressions for the diffractive response of a lossless holographic grating recorded with parameters (θ_r, θ_o, λ_r) and replayed with (θ_c, λ_c). These expressions often provide an extremely useful computational estimation of the diffractive response of many modern holographic gratings.

2.1.6. Sensitivity to wavelength and replay angle

We can understand the replay angle and wavelength behaviour of the transmission and reflection gratings by an analysis of equations (29) and (30).

To this end we assume that the illumination wave on playback is of magnitude $|k_i| = 2\pi n / \lambda_r + \Delta\beta$ and that its angle of incidence is $\theta_c = \theta_r + \Delta\theta$. Then equations (9), (11) and (27) lead to the following simple expression which relates ϑ to $\Delta\theta_c$ and $\Delta\beta$

$$\vartheta = \frac{2\pi n}{\lambda_r}\Delta\theta \sin(\theta_r - \theta_o) + \Delta\beta\{1 - \cos(\theta_r - \theta_o)\} \tag{34}$$

We will now adopt a value of $\kappa d \big/ \sqrt{c_R\,|\,c_S\,|} = \pi \big/ 2$. You may recall that this gives us perfect conversion from the R wave to the S wave in the transmission grating when $\vartheta = 0$. It also corresponds to a diffractive efficiency for the reflection hologram of 0.84. We use (29) and (30) to calculate the value of the dephasing parameter ϑ which is required to bring the diffraction to its first zero. This is given by

$$\vartheta_T = \sqrt{3}\pi\frac{c_S}{d}; \vartheta_R = \sqrt{5}\pi\frac{|\,c_S\,|}{d} \tag{35}$$

We may then use (34) to show that for the un-slanted transmission grating[2],

$$\Delta\theta_T \sim \frac{\sqrt{3}}{2}\frac{\Lambda}{d} = \frac{\sqrt{3}}{4}\frac{\lambda}{dn}\csc\theta_r \tag{36}$$

$$\left(\frac{\Delta\lambda}{\lambda}\right)_T \sim \frac{\sqrt{3}}{2}\frac{\Lambda}{d}\cot\theta_r = \frac{\sqrt{3}}{4}\frac{\lambda}{dn}\cos\theta_r \csc^2\theta_r \tag{37}$$

and for the corresponding reflection grating,

2 Note that Kogelnik gives the following formulae for the FWHM: ; .$\Delta\theta_{FWHM} = \Lambda / d$ $\Delta\lambda_{FWHM} = \cot\theta_c \cdot \Lambda / d$

$$\Delta\theta_R \sim \frac{\sqrt{5}}{2}\frac{\Lambda\cot\theta_r}{d} = \frac{\sqrt{5}}{4}\frac{\lambda}{dn}\csc\theta_r \tag{38}$$

$$\left(\frac{\Delta\lambda}{\lambda}\right)_R = \frac{\sqrt{5}}{2}\frac{\Lambda}{d} = \frac{\sqrt{5}}{4}\frac{\lambda\sec\theta_r}{dn} \tag{39}$$

This shows that a transmission grating is generally more selective in angle than a reflection grating: $\Delta\theta_R / \Delta\theta_T = \sqrt{5/3}$, independent of wavelength and angle! Similarly $\Delta\lambda_R / \Delta\lambda_T \sim \sqrt{5/3}\tan^2\theta_r$, which for small θ_r makes the reflection grating much more wavelength selective than the corresponding transmission case.

3. The PSM theory of gratings

The PSM model [3] offers an alternative method to Kogelnik's coupled wave theory for the analysis of diffraction in planar gratings. PSM stands for "Parallel Stacked Mirrors". As might be expected from this name, the theory models a holographic grating as an infinite stack of mirrors, each one parallel to the next. Each mirror is formed by a "jump" or discontinuity in the permittivity profile which constitutes the grating; the process of diffraction is then described entirely by Fresnel reflection. In many ways the PSM model can be thought of as a differential representation of the chain matrix approach of Abeles [9] as described by various authors [10,11] and which was derived from the ideas of Rouard[12]. These ideas, in turn, extend back to Darwin's 1914 work on X-ray diffraction [13]. Early attempts at an analytical formulation of diffraction in the planar grating in terms of Fresnel reflection are also due to Ludman [14] and Heifetz, Shen and Shariar [15].

3.1. The simplest model - The unslanted reflection grating at normal incidence

An unslanted holographic grating with the following index profile is assumed

$$n = n_0 + n_1\cos(\frac{4\pi n_0}{\lambda_r}y) = n_0 + \frac{n_1}{2}\left\{e^{\frac{4i\pi n_0}{\lambda_r}y} + e^{-\frac{4i\pi n_0}{\lambda_r}y}\right\} \tag{40}$$

Here, n_0 is the average index and n_1 is generally a small number representing the index modulation[3]. We can imagine that this grating was created by the interference of two counter propagating normal-incidence plane waves within a photosensitive material, each of wavelength λ_r.

Now we wish to understand the response of the grating to a plane reference wave of the form

3 Note that this is equivalent to the grating of (4) for zero slant - but note the change of coordinates.

$$R^{ext} = e^{i\beta y} \tag{41}$$

$$\text{where}\beta = \frac{2\pi n_0}{\lambda_c} \tag{42}$$

As before we shall assume that the grating is surrounded by a zone of constant index, n_0 to circumvent the complication of refraction/reflection at the grating interface. We start by modelling the grating of (40) by a series of many thin constant-index layers, $N_0, N_1, N_2, ..., N_M$, between each of which exists an index discontinuity (see Figure 4(a)). Across each such discontinuity we can derive the well-known Fresnel formulae [e.g.16] for the amplitude reflection and transmission coefficients from Maxwell's equations by demanding that the tangential components of the electric and magnetic fields be continuous. An illuminating plane wave will in general generate many mutually interfering reflections from each discontinuity. We therefore imagine two plane waves within the grating - the driving reference wave, $R(y)$ and a created signal wave, $S(y)$. Using the Fresnel formulae we may then write, for either the σ or the π-polarisation, the following relationship:

$$\begin{aligned} R_J &= 2e^{i\beta n\delta y/n_0}\left\{\frac{N_{J-1}}{N_J + N_{J-1}}\right\}R_{J-1} + e^{i\beta n\delta y/n_0}\left\{\frac{N_{J-1} - N_J}{N_J + N_{J-1}}\right\}S_J \\ S_J &= 2e^{i\beta n\delta y/n_0}\left\{\frac{N_{J+1}}{N_{J+1} + N_J}\right\}S_{J+1} + e^{i\beta n\delta y/n_0}\left\{\frac{N_{J+1} - N_J}{N_{J+1} + N_J}\right\}R_J \end{aligned} \tag{43}$$

Here the terms in brackets are just the Fresnel amplitude reflection and transmission coefficients and the exponential is a phase propagator which advances the phase of the R and S waves as they travel the distance δy between discontinuities. We now let

$$X_{J-1} = X_J - \frac{dX}{dy}\delta y - ... \tag{44}$$

and consider the limit $\delta y \to 0$. Further expanding the exponential terms as Taylor series and ignoring quadratic terms in δy we arrive at the differential counterpart to (43)

$$\begin{aligned} \frac{dR}{dy} &= \frac{R}{2}(2i\beta\frac{n}{n_0} - \frac{1}{n}\frac{dn}{dy}) - \frac{1}{2n}\frac{dn}{dy}S \\ \frac{dS}{dy} &= -\frac{S}{2}(\frac{1}{n}\frac{dn}{dy} + 2i\beta\frac{n}{n_0}) - \frac{1}{2n}\frac{dn}{dy}R \end{aligned} \tag{45}$$

These equations are an *exact* representation of Maxwell's equations for an arbitrary index profile, $n(y)$ - as letting $u(y)=R(y)-S(y)$ we see that they simply reduce to the Helmholtz equation

$$\frac{d^2u}{dy^2} + \frac{\beta^2 n^2}{n_0^2}u = 0 \tag{46}$$

and the conservation of energy

$$\frac{d}{dy}(nR^{*}R - nS^{*}S) = 0 \tag{47}$$

When $dn / dy = 0$ equations (45) describe two counter propagating and non-interacting plane waves. A finite index gradient couples these waves.

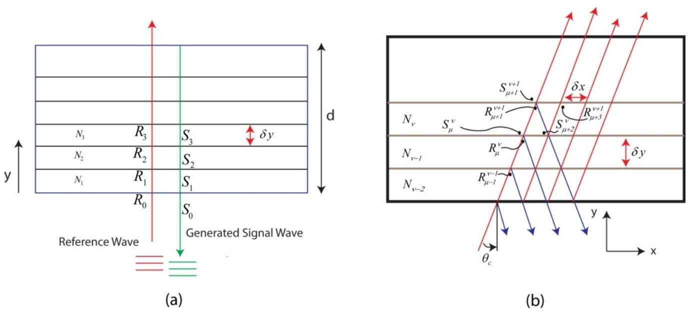

Figure 4. The PSM model of the unslanted reflection grating for (a) normal incidence and (b) for oblique incidence. In the case of normal incidence both the R and S fields have one index whereas for the case of oblique incidence the fields have two indices. In both cases the grating is modelled as a stack of dielectric layers of differing index.

We now make the transformation

$$R \to R^{'}(y)e^{i\beta y}; S \to S^{'}(y)e^{-i\beta y} \tag{48}$$

where the primed quantities are slowly varying compared to $e^{i\beta y}$. Since they are slowly-varying we can write

$$\langle R^{'} \rangle \sim R; \langle S^{'} \rangle \sim S \tag{49}$$

where the operator $\langle\rangle$ takes an average over several cycles of $e^{i\beta y}$. Substituting (48) in (45) and using (49) we then arrive at the following differential equations

$$\frac{dR}{dy} = -i\alpha\kappa S e^{2i\beta y(\alpha-1)}; \frac{dS}{dy} = i\alpha\kappa R e^{-2i\beta y(\alpha-1)} \tag{50}$$

$$\text{where}\alpha = \frac{\lambda_c}{\lambda_r} \tag{51}$$

which is just the ratio of the replay wavelength to the recording wavelength. Introducing the pseudo-field,

$$\hat{S} = S e^{2\beta i y(\alpha - 1)} \tag{52}$$

these equations may now be written in the form of Kogelnik's equations for the normal-incidence sinusoidal grating

$$c_R \frac{dR}{dy} = -i\kappa \hat{S}; c_S \frac{d\hat{S}}{dy} = -i\vartheta \hat{S} - i\kappa R \tag{53}$$

where Kogelnik's constant, κ is the same as defined previously in equation (8) but now the obliquity constants and off-Bragg parameter are a little different

$$c_R = \frac{1}{\alpha}; c_S = -\frac{1}{\alpha}; \vartheta = 2\frac{\beta}{\alpha}(1 - \alpha) \tag{54}$$

For comparison, Kogelnik's coefficients are

$$c_R = 1; c_S = (2\alpha - 1); \vartheta = 2\alpha\beta(1 - \alpha) \tag{55}$$

By imposing boundary conditions appropriate for the reflection hologram

$$R(y = 0) = 1; \hat{S}(y = d) = 0 \tag{56}$$

where d is the grating thickness, equations (53) may be solved analytically. We can then define the diffraction efficiency for both the PSM and Kogelnik models as

$$\eta = \left| \frac{c_S}{c_R} \right| \hat{S}(0)\hat{S}^*(0) = \left\{ 1 - \frac{c_R c_S}{\kappa^2}{}^2 csh^2(d) \right\}^{-1} \tag{57}$$

$$\text{where}{}^2 = -\frac{\vartheta^2}{4c_S^2} - \frac{\kappa^2}{c_R c_S} \tag{58}$$

Note that we should ensure that

$$d = m\left(\frac{\pi}{2\alpha\beta}\right) \tag{59}$$

where m is a non-zero integer to prevent a discontinuity in index at $y = d$ (see [17] for a detailed discussion of the starting and ending conditions of a grating).

For cases of practical interest for display and optical element holography, substitution of (54) (the PSM coefficients) or (55) (Kogelnik's coefficients) into (57) / (58) yield very similar results. However one should note that the only approximation made in deriving the PSM equations, (53) - (54) and (57) has been that of equation (49). This is an assumption which one would reasonably expect to hold in most gratings of interest. Equation (57) in conjunction with (55) is of course exactly equivalent to (30) for the case of zero grating slant and normal incidence.

http://dx.doi.org/10.5772/53413

At Bragg resonance, when $\alpha = 1$, both the Kogelnik and PSM models reduce to

$$\eta = \tanh^2(\kappa d) \tag{60}$$

However the PSM model provides a useful insight into what is happening within the grating: multiple reflections of the reference wave simply synthesise the signal wave by classical Fresnel reflection and transmission at each infinitesimal discontinuity. This is a rigorous picture for the normal incidence unslanted reflection grating as equations (45) are an exact representation of Maxwell's equations. The fact that we explicitly need to introduce a "pseudo-field", $\hat{S}$ in order to get the PSM equations into the same form as Kogelnik's equations reminds us that indeed Kogelnik's signal wave is not the physical electric field of the signal wave for $\alpha \neq 1$. Kogelnik's theory models the dephasing away from Bragg resonance by letting the non-physical wave propagate differently to the physical signal wave. In the PSM analytical theory (53) - (54) the pseudo-field is also not the real electric field - but here transformations (49) and (52) make the relationship between the real and the pseudo-field perfectly clear.

3.2. The unslanted panchromatic reflection grating at normal incidence

One of the advantages of the PSM model is that it does not limit the grating to a sinusoidal form. This is an advantage over the simplest variants of standard coupled-wave theories including Kogelnik's.

We start by assuming a general index profile

$$\begin{aligned} n &= n_0 + n_1\cos(2\alpha_1\beta y) + n_2\cos(2\alpha_2\beta y) + \ldots \\ &= n_0 + \frac{n_1}{2}\left\{e^{2i\beta\alpha_1 y} + e^{-2i\beta\alpha_1 y}\right\} + \frac{n_2}{2}\left\{e^{2i\beta\alpha_2 y} + e^{-2i\beta\alpha_2 y}\right\} + \ldots \end{aligned} \tag{61}$$

Equations (45) then reduce to the following form

$$\begin{aligned} \frac{dR}{dy} &= -S\sum_{j=1}^{N} i\kappa_j\alpha_j e^{2i\beta y(\alpha_j - 1)} \\ \frac{dS}{dy} &= R\sum_{j=1}^{N} i\kappa_j\alpha_j e^{-2i\beta y(\alpha_j - 1)} \end{aligned} \tag{62}$$

Assuming that the individual gratings have very different spatial frequencies these equations then lead to a simple expression for the diffractive efficiency when the reference wave is in Bragg resonance with one or another of the multiplexed gratings:

$$\eta_j = \tanh^2(\kappa_j d) \tag{63}$$

$$\text{where} \kappa_j = \frac{n_j \pi}{\lambda_c} \tag{64}$$

In addition, in the region of the j^th Bragg resonance, (62) leads to the approximate analytical form

$$\eta_j = \frac{\alpha_j{}^2 \kappa_j{}^2}{\beta^2 (1-\alpha_j)^2 + (\alpha_j{}^2 \kappa_j{}^2 - \beta^2 (1-\alpha_j)^2) coth^2 \left\{ d\sqrt{\alpha_j{}^2 \kappa_j{}^2 - \beta^2 (1-\alpha_j)^2} \right\}} \tag{65}$$

When the spatial frequencies of the different gratings are too close to one another, these relations break down. For many cases of interest however (63) to (65) provide a rather accurate picture of the normal-incidence unslanted polychromatic reflection phase grating. Indeed the following form can often be used to accurately describe an N-chromatic grating at normal incidence:

$$\eta = \sum_{j=1}^{N} \frac{\alpha_j{}^2 \kappa_j{}^2}{\beta^2 (1-\alpha_j)^2 + (\alpha_j{}^2 \kappa_j{}^2 - \beta^2 (1-\alpha_j)^2) coth^2 \left\{ d\sqrt{\alpha_j{}^2 \kappa_j{}^2 - \beta^2 (1-\alpha_j)^2} \right\}} \tag{66}$$

For example Diehl and George [18] have used a sparse Hill's matrix technique to computationally calculate the diffraction efficiency of a lossless trichromatic phase reflection grating at normal incidence. They used free-space recording wavelengths of 400nm, 500nm and 700nm. The grating thickness was 25 microns and the index parameters were taken as $n_0 = 1.5$, $n_1 = n_2 = n_3 = 0.040533$. Comparison of Equation (66) with Diehl and George's published graphical results shows very good agreement. In cases where the gratings are too close to one another in wavelength, equations (45) or (62) must, however, be solved numerically.

3.3. The unslanted reflection grating at oblique incidence

To treat the case of reference wave incidence at finite angle to the grating planes we must redraw Figure 4(a) using two-dimensional fields, *R* and *S* which we now endow with two indices instead of the previous single index (see Figure 4(b)). We shall make the approximation that the index modulation is small enough such that the rays of both the *R* and *S* waves are not deviated in angle. We shall however retain the proper Fresnel amplitude coefficients.

The Fresnel amplitude coefficients for the σ-polarisation may be written as

$$\begin{aligned} r_{k,k+1} &= \frac{N_{k+1}\sqrt{1 - \frac{n_0{}^2}{N_{k+1}{}^2}\sin^2\theta_c} - N_k\sqrt{1 - \frac{n_0{}^2}{N_k{}^2}\sin^2\theta_c}}{N_{k+1}\sqrt{1 - \frac{n_0{}^2}{N_{k+1}{}^2}\sin^2\theta_c} + N_k\sqrt{1 - \frac{n_0{}^2}{N_k{}^2}\sin^2\theta_c}} \\ t_{k,k+1} &= \frac{2N_k\sqrt{1 - \frac{n_0{}^2}{N_k{}^2}\sin^2\theta_c}}{N_{k+1}\sqrt{1 - \frac{n_0{}^2}{N_{k+1}{}^2}\sin^2\theta_c} + N_k\sqrt{1 - \frac{n_0{}^2}{N_k{}^2}\sin^2\theta_c}} \end{aligned} \tag{67}$$

where r and t pertain respectively to reflection and transmission occurring at the index discontinuity between layers k and k+1. The R and S waves in the exterior medium of index n_0 are assumed to be plane waves of the form

$$R = e^{i(k_{cx}x + k_{cy}y)};\ S = S_0 e^{i(k_{ix}x + k_{iy}y)} \tag{68}$$

where S_0 is a constant. Within the grating we shall assume that R and S are functions of x and y. Using the normal rules of Fresnel reflection, the wave-vectors can be written explicitly as

$$\boldsymbol{k_c} = \beta\begin{pmatrix}\sin\theta_c\\ \cos\theta_c\end{pmatrix};\ \boldsymbol{k}_i = \beta\begin{pmatrix}\sin\theta_c\\ -\cos\theta_c\end{pmatrix} \tag{69}$$

where the angle θ_c is the angle of incidence of the R wave.

We can now use Figure 4 (b) to write down two expressions relating the discrete values of R and S within the grating. These are an equation for $R_{\mu+1}^{\nu+1}$

$$\begin{aligned}R_{\mu+1}^{\nu+1} = {} & e^{i\beta n(\sin\theta_c\delta x + \cos\theta_c\delta y)/n_0} R_\mu^\nu \left\{\frac{2N_{\nu-1}\sqrt{1-\frac{n_0^2}{N_{\nu-1}^2}\sin^2\theta_c}}{N_{\nu-1}\sqrt{1-\frac{n_0^2}{N_{\nu-1}^2}\sin^2\theta_c} + N_\nu\sqrt{1-\frac{n_0^2}{N_\nu^2}\sin^2\theta_c}}\right\}\\ & + e^{i\beta n(\sin\theta_c\delta x + \cos\theta_c\delta y)/n_0} S_\mu^\nu \left\{\frac{N_{\nu-1}\sqrt{1-\frac{n_0^2}{N_{\nu-1}^2}\sin^2\theta_c} - N_\nu\sqrt{1-\frac{n_0^2}{N_\nu^2}\sin^2\theta_c}}{N_{\nu-1}\sqrt{1-\frac{n_0^2}{N_{\nu-1}^2}\sin^2\theta_c} + N_\nu\sqrt{1-\frac{n_0^2}{N_\nu^2}\sin^2\theta_c}}\right\}\end{aligned} \tag{70}$$

and the corresponding equation for $S_{\mu+1}^{\nu-1}$

$$\begin{aligned}S_{\mu+1}^{\nu-1} = {} & e^{i\beta n(\sin\theta_c\delta x + \cos\theta_c\delta y)/n_0} S_\mu^\nu \left\{\frac{2N_\nu\sqrt{1-\frac{n_0^2}{N_\nu^2}\sin^2\theta_c}}{N_{\nu-1}\sqrt{1-\frac{n_0^2}{N_{\nu-1}^2}\sin^2\theta_c} + N_\nu\sqrt{1-\frac{n_0^2}{N_\nu^2}\sin^2\theta_c}}\right\}\\ & + e^{i\beta n(\sin\theta_c\delta x + \cos\theta_c\delta y)/n_0} R_\mu^\nu \left\{\frac{N_\nu\sqrt{1-\frac{n_0^2}{N_\nu^2}\sin^2\theta_c} - N_{\nu-1}\sqrt{1-\frac{n_0^2}{N_{\nu-1}^2}\sin^2\theta_c}}{N_{\nu-1}\sqrt{1-\frac{n_0^2}{N_{\nu-1}^2}\sin^2\theta_c} + N_\nu\sqrt{1-\frac{n_0^2}{N_\nu^2}\sin^2\theta_c}}\right\}\end{aligned} \tag{71}$$

Since we are assuming that δx and δy are small we can use Taylor expansions for the fields and index profile

$$
\begin{aligned}
R_{\mu+1}^{\nu+1} &= R_{\mu}^{\nu} + \frac{\partial R_{\mu}^{\nu}}{\partial x}\delta x + \frac{\partial R_{\mu}^{\nu}}{\partial y}\delta y + \ldots \\
S_{\mu+1}^{\nu-1} &= S_{\mu}^{\nu} + \frac{\partial S_{\mu}^{\nu}}{\partial x}\delta x - \frac{\partial S_{\mu}^{\nu}}{\partial y}\delta y + \ldots \\
N_{\nu-1} &= N_{\nu} - \frac{\partial N_{\nu}}{\partial y}\delta y + \ldots
\end{aligned} \tag{72}
$$

The exponentials are also written using a Taylor expansion. Then using the following additional approximations

$$
\sqrt{1-\frac{n_0{}^2}{N_\nu{}^2}\sin^2\theta_c} = \sqrt{1-\frac{a}{N_\nu{}^2}} \sim \cos\theta_c = b \tag{73}
$$

$$
\sqrt{1-\frac{n_0{}^2}{N_{\nu-1}{}^2}\sin^2\theta_c} \sim b - \frac{\partial N_\nu}{\partial y}\frac{a\delta y}{bN_\nu^3} + O(\delta y^2) \tag{74}
$$

$$
\text{letting} R_\mu^\nu \to R; S_\mu^\nu \to S; N_\nu \to n \tag{75}
$$

and taking the limit $\delta x,\ \delta y \to 0$, we arrive at partial differential equations for the $R$and S fields

$$
\frac{\boldsymbol{k_c}}{\beta}\cdot\nabla R = \sin\theta_c\frac{\partial R}{\partial x} + \cos\theta_c\frac{\partial R}{\partial y} = \frac{R}{2}\left\{2i\beta - \frac{1}{n\cos\theta_c}\frac{\partial n}{\partial y}\right\} - \frac{S}{2n\cos\theta_c}\frac{\partial n}{\partial y} \tag{76}
$$

$$
\frac{\boldsymbol{k_i}}{\beta}\cdot\nabla S = \sin\theta_c\frac{\partial S}{\partial x} - \cos\theta_c\frac{\partial S}{\partial y} = \frac{S}{2}\left\{2i\beta + \frac{1}{n\cos\theta_c}\frac{\partial n}{\partial y}\right\} + \frac{R}{2n\cos\theta_c}\frac{\partial n}{\partial y} \tag{77}
$$

Note the similarity of (76) and (77) to (45). Note also that if we set $\theta_c=0$ then we retrieve (45) exactly. Equations (76) and (77) are the PSM equations for an unslanted reflection grating at oblique incidence for the σ-polarisation. Corresponding equations can be derived for the π-polarisation by consideration of the appropriate Fresnel reflection formulae [e.g.16]. These give

$$
\frac{\boldsymbol{k_c}}{\beta}\cdot\nabla R = \sin\theta_c\frac{\partial R}{\partial x} + \cos\theta_c\frac{\partial R}{\partial y} = \frac{R}{2}\left\{2i\beta - \frac{1}{n}\frac{\cos2\theta_c}{\cos\theta_c}\frac{\partial n}{\partial y}\right\} - \frac{S}{2n}\frac{\cos2\theta_c}{\cos\theta_c}\frac{\partial n}{\partial y} \tag{78}
$$

$$
\frac{\boldsymbol{k_i}}{\beta}\cdot\nabla S = \sin\theta_c\frac{\partial S}{\partial x} - \cos\theta_c\frac{\partial S}{\partial y} = \frac{S}{2}\left\{2i\beta + \frac{1}{n}\frac{\cos2\theta_c}{\cos\theta_c}\frac{\partial n}{\partial y}\right\} + \frac{R}{2n}\frac{\cos2\theta_c}{\cos\theta_c}\frac{\partial n}{\partial y} \tag{79}
$$

3.3.1. Simplification of the PSM equations to ODEs

The PSM equations may be simplified under boundary conditions corresponding to monochromatic illumination of the grating.

Let

$$R \to R(y)e^{i\beta \sin\theta_c x}; S \to S(y)e^{i\beta \sin\theta_c x} \tag{80}$$

Under this transformation equations (76) - (77) yield the following pair of ordinary differential equations

$$\begin{aligned} \cos\theta_c \frac{dR}{dy} &= \frac{R}{2}\left\{2i\beta\cos^2\theta_c - \frac{1}{n\cos\theta_c}\frac{dn}{dy}\right\} - \frac{S}{2}\left\{\frac{1}{n\cos\theta_c}\frac{dn}{dy}\right\} \\ -\cos\theta_c \frac{dS}{dy} &= \frac{S}{2}\left\{2i\beta\cos^2\theta_c + \frac{1}{n\cos\theta_c}\frac{dn}{dy}\right\} + \frac{R}{2}\left\{\frac{1}{n\cos\theta_c}\frac{dn}{dy}\right\} \end{aligned} \tag{81}$$

Similarly the π-polarisation equations yield

$$\begin{aligned} \cos\theta_c \frac{dR}{dy} &= \frac{R}{2}\left\{2i\beta\cos^2\theta_c - \frac{\cos 2\theta_c}{n\cos\theta_c}\frac{dn}{dy}\right\} - \frac{S}{2}\left\{\frac{\cos 2\theta_c}{n\cos\theta_c}\frac{dn}{dy}\right\} \\ -\cos\theta_c \frac{dS}{dy} &= \frac{S}{2}\left\{2i\beta\cos^2\theta_c + \frac{\cos 2\theta_c}{n\cos\theta_c}\frac{dn}{dy}\right\} + \frac{R}{2}\left\{\frac{\cos 2\theta_c}{n\cos\theta_c}\frac{dn}{dy}\right\} \end{aligned} \tag{82}$$

Equations (81) and (82) are approximate only because we have assumed an approximate form for the direction vector of the waves within the grating. We may however approach the problem differently and derive exact equations directly from (45). For example, in the case of the σ-polarisation, we use the optical invariant

$$\tilde{\beta}(y) \to \tilde{\beta}(y)\cos\theta(y) \tag{83}$$

$$\text{where} \tilde{\beta}(y) = \frac{\beta n(y)}{n_0} \tag{84}$$

Then using Snell's law

$$\frac{d\tilde{\beta}(y)}{dy}\sin\theta(y) + \tilde{\beta}(y)\frac{d\theta(y)}{dy}\cos\theta(y) = 0 \tag{85}$$

it is simple to see that (45) reduces to

$$\begin{aligned} \cos\theta\frac{dR}{dy} &= \frac{R}{2}\left\{2i\beta\cos^2\theta - \frac{1}{\beta\cos\theta}\frac{d\beta}{dy}\right\} - \frac{S}{2}\left\{\frac{1}{\beta\cos\theta}\frac{d\beta}{dy}\right\} \\ -\cos\theta\frac{dS}{dy} &= \frac{S}{2}\left\{2i\beta\cos^2\theta + \frac{1}{\beta\cos\theta}\frac{d\beta}{dy}\right\} + \frac{R}{2}\left\{\frac{1}{\beta\cos\theta}\frac{d\beta}{dy}\right\} \end{aligned} \tag{86}$$

where θ is now a function of y throughout the grating. If we now replace (80) with the more general behaviour

$$R \to R(y)e^{i\beta(y)\sin\theta(y)x}; S \to S(y)e^{i\beta(y)\sin\theta(y)x} \tag{87}$$

then (86) is seen to be an exact solution of the Helmholtz equation. Therefore the solution of (85) and (86) subject to the boundary conditions (56) and $\theta(0)=\theta_c$ constitute a rigorous solution of the Helmholtz equation. Note that this is independent of periodicity required by a Floquet solution. Since these equations are none other than a differential representation of the chain matrix method of thin films [11], it is simple to show that this implies that the chain matrix method is itself rigorous.

3.3.2. Analytic solutions for sinusoidal gratings

We start by defining an unslanted grating with the following index profile

$$n = n_0 + n_1\cos(2\alpha\beta\cos\theta_r y) = n_0 + \frac{n_1}{2}\left\{e^{2i\alpha\beta\cos\theta_r y} + e^{-2i\alpha\beta\cos\theta_r y}\right\} \tag{88}$$

where we imagine θ_r to be the recording angle of this grating. Then letting

$$R \to R(y)e^{i\beta\cos\theta_c y}; S \to S(y)e^{-i\beta\cos\theta_c y} \tag{89}$$

and using (49), equations (81) reduce to

$$\begin{aligned} \cos\theta_c\frac{dR}{dy} &= -\frac{1}{2n}n_1 i\beta\alpha\frac{\cos\theta_r}{\cos\theta_c}\left\langle\left\{e^{2i\beta\alpha\cos\theta_r y} + \ldots\right\}Se^{-2i\beta y\cos\theta_c}\right\rangle \\ &= -\frac{n_1 i\beta(\alpha\cos\theta_r)}{2n\cos\theta_c}Se^{2i\beta y(\alpha\cos\theta_r - \cos\theta_c)} \\ \cos\theta_c\frac{dS}{dy} &= \frac{1}{2n}n_1 i\beta\alpha\frac{\cos\theta_r}{\cos\theta_c}\left\langle\left\{e^{-2i\beta\alpha\cos\theta_r y} + \ldots\right\}Re^{2i\beta y\cos\theta_c}\right\rangle \\ &= \frac{n_1 i\beta(\alpha\cos\theta_r)}{2n\cos\theta_c}Re^{-2i\beta y(\alpha\cos\theta_r - \cos\theta_c)} \end{aligned} \tag{90}$$

As before we now define the pseudo-field

$$\hat{S} = S e^{2i\beta y(\alpha\cos\theta_r - \cos\theta_c)} \tag{91}$$

whereupon equations (90) reduce to the standard form of Kogelnik's equations

$$c_R \frac{dR}{dy} = -i\kappa\hat{S}; c_S \frac{d\hat{S}}{dy} = -i\vartheta\hat{S} - i\kappa R \tag{92}$$

The coefficients for the PSM model and for Kogelnik's model are as follows:

$$\begin{aligned}
&c_{R(PSM)} = \frac{\cos^2\theta_c}{\alpha\cos\theta_r} c_{R(KOG)} = \cos\theta_c \\
&c_{S(PSM)} = -\frac{\cos^2\theta_c}{\alpha\cos\theta_r} c_{S(KOG)} = \cos\theta_c - 2\alpha\cos\theta_r \\
&\vartheta_{PSM} = 2\beta(1 - \frac{\cos\theta_c}{\alpha\cos\theta_r})\cos^2\theta_c \vartheta_{KOG} = 2\alpha\beta\cos\theta_r(\cos\theta_c - \alpha\cos\theta_r)
\end{aligned} \tag{93}$$

Equations (92) in conjunction with the boundary conditions (56) then lead, as before to the general analytic expression for the diffractive efficiency of the unslanted reflection grating:

$$\eta_\sigma = \frac{|c_S|}{c_R}\hat{S}(0)\hat{S}^*(0) = \frac{\kappa^2\sinh^2(d)}{\kappa^2\sinh^2(d) - c_R c_S{}^2} \tag{94}$$

$$\text{where}\ ^2 = -\frac{\vartheta^2}{4c_S{}^2} - \frac{\kappa^2}{c_R c_S} \tag{95}$$

Note that at Bragg resonance both the PSM theory and Kogelnik's theory reduce to the well-known formula

$$\eta_\sigma = \tanh^2(\kappa d\sec\theta_c) \tag{96}$$

The π-polarisation may be treated in an exactly analogous way, leading to the following pair of ordinary differential equations for R and $\hat{S}$:

$$c_R \frac{dR}{dy} = -i\kappa\cos2\theta_c\hat{S}; c_S \frac{d\hat{S}}{dy} = -i\vartheta\hat{S} - i\kappa\cos2\theta_c R \tag{97}$$

These are just Kogelnik's equations with a modified κ parameter. The PSM model distinguishes the π and σ-polarisations in exactly the same manner as Kogelnik's theory does! In both theories, in the case of the unslanted grating, Kogelnik's constant is simply transformed according to the rule

$$|\kappa| \rightarrow |\kappa\cos 2\theta_c| \tag{98}$$

The practical predictions of Kogelnik's model and the PSM model are very close for gratings of interest to display and optical element holography. This is largely due to the effect of Snell's law which acts to steepen the angle of incidence in most situations. But at very high angles of incidence within the grating, larger differences appear.

3.3.3. Multi-colour gratings

A multi-colour unslanted reflection grating can be modelled in the following way

$$\begin{aligned} n &= n_0 + n_1\cos(2\alpha_1\beta\cos\theta_{r1}y) + n_2\cos(2\alpha_2\beta\cos\theta_{r2}y) + \ldots \\ &= n_0 + \frac{1}{2}\sum_{j=1}^{N} n_j\left\{e^{2i\alpha_j\beta\cos\theta_{rj}y} + e^{-2i\alpha_j\beta\cos\theta_{rj}y}\right\} \end{aligned} \tag{99}$$

In this case the PSM σ-polarisation equations yield

$$\begin{aligned} \cos\theta_c\frac{dR}{dy} &= -S\sum_{j=1}^{N} i\kappa_j\alpha_j\frac{\cos\theta_{rj}}{\cos\theta_c}e^{2i\beta y(\alpha_j\cos\theta_{rj}-\cos\theta_c)} \\ \cos\theta_c\frac{dS}{dy} &= R\sum_{j=1}^{N} i\kappa_j\alpha_j\frac{\cos\theta_{rj}}{\cos\theta_c}e^{-2i\beta y(\alpha_j\cos\theta_{rj}-\cos\theta_c)} \end{aligned} \tag{100}$$

$$\text{where}\kappa_j = \frac{n_j\pi}{\lambda_c} \tag{101}$$

Once again, if we assume that the individual gratings have very different spatial frequencies, then these equations lead to a simple expression for the diffractive efficiency when the reference wave is in Bragg resonance with one or another of the multiplexed gratings:

$$\eta_{PSM/\sigma_j} = \tanh^2(\kappa_j d\sec\theta_c) \tag{102}$$

The corresponding result for the π-polarisation is

$$\eta_{PSM/\pi_j} = \tanh^2(\kappa_j d\sec\theta_c\cos 2\theta_c) \tag{103}$$

In the region of the j$^{\text{th}}$ Bragg resonance, (100) leads to the approximate analytical form[4]

$$\eta_{\sigma j} = \frac{\kappa_{\sigma j}{}^2\sinh^2(d_{\sigma j})}{\kappa_{\sigma j}{}^2\sinh^2(d_{\sigma j}) - c_R c_{S\sigma j}{}^2} \tag{104}$$

4 Note that the ${}_{\sigma j}^{2} = -\frac{\vartheta_{\sigma j}^2}{4c_S{}^2} - \frac{\kappa_j{}^2}{c_R c_S}$ and $\vartheta_{\sigma j} = 2\beta(1 - \frac{\cos\theta_c}{\alpha_j\cos\theta_r})\cos^2\theta_c$

Again, as long as there is sufficient difference in the spatial frequencies of each grating we can add each response to give an convenient analytical expression for the total diffraction efficiency:

$$\eta_\sigma = \sum_{j=1}^{N} \frac{\kappa_{\sigma j}{}^2 \sinh^2(d_{\sigma j})}{\kappa_{\sigma j}{}^2 \sinh^2(d_{\sigma j}) - c_R c_{S\sigma j}{}^2} \tag{105}$$

In cases where the individual gratings are too close to one another in wavelength or where small amplitude interaction effects between gratings are to be described, equations (100) must be solved numerically.

3.4. The slanted reflection grating at oblique incidence

We may use the PSM equations for the unslanted grating to derive corresponding equations for the general slanted grating. To do this we define rotated Cartesian coordinates (x', y') which are related to the un-primed Cartesian system by

$$\begin{pmatrix} x' \\ y' \end{pmatrix} = \begin{pmatrix} \cos\psi & -\sin\psi \\ \sin\psi & \cos\psi \end{pmatrix} \begin{pmatrix} x \\ y \end{pmatrix} \tag{106}$$

In the un-primed frame we have

$$\boldsymbol{k_c} = \beta \begin{pmatrix} \sin\theta_c \\ \cos\theta_c \end{pmatrix}; \boldsymbol{k}_i = \beta \begin{pmatrix} \sin\theta_c \\ -\cos\theta_c \end{pmatrix} \tag{107}$$

whereas in the primed frame we have

$$\boldsymbol{k}'_c = \beta \begin{pmatrix} \sin(\theta_c - \psi) \\ \cos(\theta_c - \psi) \end{pmatrix}; \boldsymbol{k}'_i = \beta \begin{pmatrix} \sin(\theta_c + \psi) \\ -\cos(\theta_c + \psi) \end{pmatrix} \tag{108}$$

Derivatives in the primed system are related to those in the un-primed system by Leibnitz's chain rule

$$\begin{aligned} \frac{\partial}{\partial x} &= \frac{\partial x'}{\partial x}\frac{\partial}{\partial x'} + \frac{\partial y'}{\partial x}\frac{\partial}{\partial y'} = \cos\psi \frac{\partial}{\partial x'} + \sin\psi \frac{\partial}{\partial y'} \\ \frac{\partial}{\partial y} &= \frac{\partial y'}{\partial y}\frac{\partial}{\partial y'} + \frac{\partial x'}{\partial y}\frac{\partial}{\partial x'} = -\sin\psi \frac{\partial}{\partial x'} + \cos\psi \frac{\partial}{\partial y'} \end{aligned} \tag{109}$$

The PSM equations for the σ-polarisation may therefore be written as

$$\frac{\boldsymbol{k}'_c}{\beta} \cdot \nabla' R = \frac{\partial R}{\partial x'}\sin(\theta_c - \psi) + \frac{\partial R}{\partial y'}\cos(\theta_c - \psi) = \frac{R}{2}\left\{2i\beta - \frac{1}{n\cos\theta_c}\frac{\partial n}{\partial y}\right\} - \frac{S}{2n\cos\theta_c}\frac{\partial n}{\partial y} \tag{110}$$

and

$$\frac{\boldsymbol{k}'_i}{\beta}\cdot\nabla' S=\frac{\partial S}{\partial x'}\sin(\theta_c+\psi)-\frac{\partial S}{\partial y'}\cos(\theta_c+\psi)=\frac{S}{2}\left\{2i\beta+\frac{1}{n\cos\theta_c}\frac{\partial n}{\partial y}\right\}+\frac{R}{2n\cos\theta_c}\frac{\partial n}{\partial y} \tag{111}$$

Note that we have kept the un-primed frame on the RHS on purpose as in this system the index profile is one dimensional and so much easier to evaluate.

3.4.1. Analytic solutions for sinusoidal gratings

To study the single colour grating we use the unslanted index profile (88) in the un-primed frame leading to the following profile in the primed frame

$$\begin{aligned} n&=n_0+n_1\cos(2\alpha\beta\cos\theta_r\{\sin\psi x'-\cos\psi y'\})\\ &=n_0+\frac{n_1}{2}\left\{e^{2i\beta\alpha\cos\theta_r\hat{\boldsymbol{K}}.\boldsymbol{r}'}+e^{-2i\beta\alpha\cos\theta_r\hat{\boldsymbol{K}}.\boldsymbol{r}'}\right\}\end{aligned} \tag{112}$$

Letting

$$R\rightarrow \mathrm{R}e^{i\beta\{\sin(\theta_c-\psi)x'+\cos(\theta_c-\psi)y'\}};S\rightarrow Se^{i\beta\{\sin(\theta_c+\psi)x'-\cos(\theta_c+\psi)y'\}} \tag{113}$$

Equations (110) and (111) then become

$$\begin{aligned}&\sin(\theta_c-\psi)\frac{\partial R}{\partial x'}+\cos(\theta_c-\psi)\frac{\partial R}{\partial y'}\\ &=-\frac{S}{2}\left\{\frac{1}{n\cos\theta_c}\frac{\partial n}{\partial y}\right\}e^{i\beta\{[\sin(\theta_c+\psi)-\sin(\theta_c-\psi)]x'-[\cos(\theta_c-\psi)+\cos(\theta_c+\psi)]y'\}}\\ &=-\frac{S}{2}\left\langle\left\{\frac{1}{n_0\cos\theta_c}\frac{\partial}{\partial y}\frac{n_1}{2}\left\{e^{2i\beta\alpha(\cos\theta_r)y}+e^{-2i\beta\alpha(\cos\theta_r)y}\right\}\right\}e^{2i\beta\cos\theta_c\{[\sin\psi]x'-[\cos\psi]y'\}}\right\rangle\\ &=-\frac{i\beta n_1}{2n_0}\alpha\frac{\cos\theta_r}{\cos\theta_c}Se^{2i\beta(\alpha\cos\theta_r-\cos\theta_c)(y'\cos\psi-x'\sin\psi)}\end{aligned} \tag{114}$$

$$\text{and}\sin(\theta_c+\psi)\frac{\partial S}{\partial x'}-\cos(\theta_c+\psi)\frac{\partial S}{\partial y'}=-\frac{i\beta n_1}{2n_0}\alpha\frac{\cos\theta_r}{\cos\theta_c}Re^{-2i\beta(\alpha\cos\theta_r-\cos\theta_c)(y'\cos\psi-x'\sin\psi)} \tag{115}$$

Next we make the transformation

$$\hat{S}=S(y')e^{2i\beta(\alpha\cos\theta_r-\cos\theta_c)(y'\cos\psi-x'\sin\psi)};\hat{R}=R(y') \tag{116}$$

whereupon once again the PSM equations reduce to a simple pair of ordinary differential equations of the form of Kogelnik's equations, (92) with coefficients

http://dx.doi.org/10.5772/53413

$$c_{R(PSM)} = \frac{\cos\theta_c \cos(\theta_c - \psi)}{\alpha\cos\theta_r}; c_{S(PSM)} = -\frac{\cos\theta_c \cos(\theta_c + \psi)}{\alpha\cos\theta_r}; \vartheta_{PSM} = 2\beta(1 - \frac{\cos\theta_c}{\alpha\cos\theta_r})\cos^2\theta_c \quad (117)$$

For comparison, Kogelnik's coefficients are

$$c_{R(KOG)} = \cos(\theta_c - \psi); c_{S(KOG)} = \cos(\theta_c - \psi) - 2\alpha\cos\theta_r\cos\psi; \vartheta_{KOG} = 2\alpha\beta\cos\theta_r(\cos\theta_c - \alpha\cos\theta_r) \quad (118)$$

With the usual reflective boundary conditions $\hat{R}(0)=1$ and $\hat{S}(d)=0$ we can then use the standard formula to describe the diffraction efficiency of the slanted reflection grating:

$$\eta_\sigma = \frac{|\, c_S \,|}{c_R}\hat{S}(0)\hat{S}^*(0) = \frac{\kappa^2 \sinh^2(d)}{\kappa^2 \sinh^2(d) - c_R {c_S}^2} \quad (119)$$

$$\text{where}\,^2 = -\frac{\vartheta^2}{4{c_S}^2} - \frac{\kappa^2}{c_R c_S} \quad (120)$$

Substitution of either (117) or (118) into (119) gives the required expression for the diffractive efficiency in either the Kogelnik or PSM model. When $\psi=0$, $\eta_{PSM/\sigma}$ reduces to the un-slanted formula which was derived in section 3.3.2. In the case of finite slant and Bragg resonance (where $\cos\theta_c = \alpha\cos\theta_r$) we have

$$\eta_{PSM/\sigma} = \tanh^2(d\kappa\sqrt{\sec(\theta_c - \psi)\sec(\theta_c + \psi)}) \quad (121)$$

which is identical to Kogelnik's solution. Note that the behaviour of the π-polarisation is simply described by making the transformation (98) in all formulae of interest. The PSM model for the slanted grating under either the σ or π polarisations gives expressions very similar to Kogelnik's theory. For most gratings of practical interest to display and optical element holography, the two theories produce predictions which are extremely close.

3.4.2. Polychromatic gratings

As before the formulae (102) - (105) with coefficients (117) give useful expressions for the diffractive efficiency of the general polychromatic slanted reflection grating at oblique incidence.

3.5. Slanted transmission gratings at oblique incidence

The PSM model can be applied to transmission gratings by simply using the appropriate boundary conditions to solve the PSM equations in a rotated frame. We use the transmission boundary conditions

$$R(0)=1; S(0)=0 \quad (122)$$

to solve equations (92) with coefficients (117) which at Bragg resonance result in the standard formula given by Kogelnik's theory.

$$\eta_{\sigma T/PSM} = \sin^2(\kappa d / \sqrt{c_R c_S}) = \sin^2(\kappa d / \sqrt{-\cos(\theta_c - \psi)\cos(\theta_c + \psi)}) \tag{123}$$

4. Theory of the spatially-multiplexed reflection grating

Both Kogelnik's Coupled wave model and the PSM model can be extended to model diffraction from spatially multiplexed gratings of the form [19]

$$\begin{aligned} n &= n_0 + \sum_{\mu=1}^{N} n_\mu \cos(2\alpha\beta\cos\theta_{r\mu}\{\sin\psi_\mu x' - \cos\psi_\mu y'\}) \\ &= n_0 + \sum_{\mu=1}^{N} \frac{n_\mu}{2}\{e^{i\mathbf{K}_\mu.\mathbf{r}'} + e^{-i\mathbf{K}_\mu.\mathbf{r}'}\} \end{aligned} \tag{124}$$

In PSM this is done by considering the Fresnel reflections from N grating planes, each having a slant ψ_μ, and assuming that cross-reflections between grating planes do not add up to a significant amplitude. This leads to the N-PSM equations for the spatially multiplexed monochromatic grating

$$\frac{\partial R}{\partial y'} = -i\sum_{\mu=1}^{N} \frac{\kappa_\mu}{c_{R\mu}} \hat{S}_\mu ; c_{S\mu} \frac{\partial \hat{S}_\mu}{\partial y'} = -i\vartheta_\mu \hat{S}_\mu - i\kappa_\mu R \tag{125}$$

where for the σ-polarisation

$$c_{R\mu} = \frac{\cos\theta_{c\mu}\cos(\theta_{c\mu} - \psi_\mu)}{\alpha\cos\theta_{r\mu}} ; c_{S\mu} = -\frac{\cos\theta_{c\mu}\cos(\theta_{c\mu} + \psi_\mu)}{\alpha\cos\theta_{r\mu}} ; \vartheta_\mu = 2\beta(1 - \frac{\cos\theta_{c\mu}}{\alpha\cos\theta_{r\mu}})\cos^2\theta_{c\mu} \tag{126}$$

and where

$$\left.\begin{aligned} \theta_{c\mu} - \psi_\mu = \Phi_c ; \theta_{c\mu} + \psi_\mu = -\Phi_{i\mu} \\ \theta_{r\mu} - \psi_\mu = \Phi_r ; \theta_{r\mu} + \psi_\mu = -\Phi_{o\mu} \end{aligned}\right\} \forall \mu \le N \tag{127}$$

Here the θ variables indicate incidence angles with respect to the respective grating plane normals and the Φ variables indicate incidence angles with respect to the physical normal of the grating. These equations may be solved using the boundary conditions appropriate for a reflection multiplexed grating - i.e.

$$R(0) = 1; \hat{S}_\mu(d) = 0 \forall \mu \le N \tag{128}$$

At Bragg resonance $c_{R\mu}$ becomes a constant

$$c_R = c_{R\mu} = \frac{\cos\theta_{c\mu}\cos(\theta_{c\mu} - \psi_\mu)}{\alpha_\mu \cos\theta_{r\mu}} = \cos\Phi_c \tag{129}$$

and (125) then gives the following expression for the diffractive efficiency of the μ^{th} grating:

$$\eta_\mu \equiv \frac{1}{c_R} \mid c_{s\mu} \mid \hat{S}_\mu(0)\hat{S}_\mu{}^*(0) = \frac{1}{c_{s\mu}} \frac{\kappa_\mu^2}{\sum_{k=1}^{N} \frac{\kappa_k^2}{c_{sk}}} \tanh^2\left\{ d\sqrt{-\frac{1}{c_R}\sum_{k=1}^{N} \frac{\kappa_k^2}{c_{sk}}} \right\} \tag{130}$$

The total diffraction efficiency of the entire multiplexed grating is likewise found by summing the diffractive response from each grating:

$$\eta \equiv \sum_{\mu=1}^{N} \eta_\mu = \tanh^2\left\{ d\sqrt{\frac{1}{\cos\Phi_c}\sum_{k=1}^{N} \frac{\kappa_k^2}{\cos\Phi_{ik}}} \right\} \tag{131}$$

Here Φ_c is the incidence angle of the replay reference wave and Φ_{ik} is the incidence angle of the k$^{\text{th}}$ signal wave. These results are identical to the expressions obtained from an extension of Kogelnik's theory - the N-coupled wave theory of Solymar and Cooke [2]. At Bragg resonance the N-PSM model of the multiplexed grating therefore gives an identical description to the corresponding N-coupled wave theory just as the simple PSM theory gives an identical description at Bragg resonance to Kogelnik's theory. Away from Bragg resonance however, the predictions of the two models will be somewhat different.

N-PSM can be extended to the polychromatic case in which case (130) generalises to

$$\eta_{mj} \equiv \frac{1}{c_{sj}} \frac{\kappa_{mj}^2}{\sum_{k=1}^{N} \frac{\kappa_{mk}^2}{c_{sk}}} \tanh^2\left\{ d\sqrt{-\frac{1}{c_R}\sum_{k=1}^{N} \frac{\kappa_{mk}^2}{c_{sk}}} \right\} \tag{132}$$

In the limit that $N \rightarrow \infty$ the above results also lead to formulae for the diffractive efficiency of the lossless polychromatic reflection hologram

$$\begin{aligned} \eta_m(\Phi_c, \Phi_i) &= \frac{\kappa_m^2(\Phi_i)}{L_m \cos\Phi_i} \tanh^2\left\{ d\sqrt{\frac{L_m}{\cos\Phi_c}} \right\} \\ \eta_m &= \frac{1}{\Delta\Phi}\int \frac{\kappa_m^2(\Phi')}{L_m \cos\Phi'} \tanh^2\left\{ d\sqrt{\frac{L_m}{\cos\Phi_c}} \right\} d\Phi' = \tanh^2\left\{ d\sqrt{\frac{L_m}{\cos\Phi_c}} \right\} \end{aligned} \tag{133}$$

$$\text{where} L_m = \frac{1}{\Delta\Phi}\int \frac{\kappa_m^2(\Phi)}{\cos\Phi} d\Phi \tag{134}$$

and where Φ is the replay image angle and $\Delta\Phi$ is the total reconstructed image angle range.

5. Rigorous coupled wave theory

Moharam and Gaylord [5] first showed how coupled wave theory could be formulated without approximation. This led to a computational algorithm which could be used to solve the wave equation exactly. Although earlier approaches such as the Modal method [20] were also rigorous they involved the solution of a trancendental equation for which a general unique algorithm could not be defined. This contrasted to the simple Eigen formulation of Maraham and Gaylord. Here we provide a derivation of rigorous coupled wave theory for the more complicated spatially multiplexed case. For brevity we shall limit discussions to the σ-polarisation for which the Helmholtz equation may be written

$$\frac{\partial^2 u}{\partial x^2}+\frac{\partial^2 u}{\partial y^2}-\gamma^2 u=0 \tag{135}$$

where u is the transverse (z) electric field and the parameter

$$\gamma^2=-\beta^2-2\beta\sum_{\mu=1}^{N}\kappa_\mu\left\{e^{i\boldsymbol{K}_\mu\cdot\boldsymbol{r}}+e^{-i\boldsymbol{K}_\mu\cdot\boldsymbol{r}}\right\} \tag{136}$$

defines the multiplexed grating[5]. We consider the case of illumination of the grating by a wave of the form

$$u(y<0)=e^{i(k_x x+k_y y)} \tag{137}$$

$$\text{where}\begin{array}{l}k_x=\beta\sin(\theta_{c\mu}-\psi_\mu)\\ k_y=\beta\cos(\theta_{c\mu}-\psi_\mu)\end{array}\forall\,\mu \tag{138}$$

In both the front region $(y<0)$ and the rear region $(y<d)$ the average index is assumed to be n_0. Now the Helmholtz field, $u(x,\ y)$ may be consistently expanded in the following way

$$\begin{aligned}u(x,\ y)&=\sum_{l_1=-\infty}^{\infty}\sum_{l_2=-\infty}^{\infty}\sum_{l_3=-\infty}^{\infty}\ldots u_{l_1l_2l_3\ldots}(y)e^{i(k_x+l_1K_{1x}+l_2K_{2x}+\ldots)x}\\&=\sum_{l_1=-\infty}^{\infty}\sum_{l_2=-\infty}^{\infty}\sum_{l_3=-\infty}^{\infty}\ldots u_{l_1l_2l_3\ldots}(y)e^{ik_x x}\prod_{\sigma=1}^{N}e^{il_\sigma K_{\sigma x}x}\end{aligned} \tag{139}$$

5 This is just the same as (124)

This expression may be substituted into (135) and(136). On taking the Fourier transform and applying orthogonality we then arrive at the following rigorous coupled wave equations:

$$\begin{aligned}&\left\{(k_x+\sum_{\sigma=1}^{N} l_\sigma K_{\sigma x})^2-\beta^2\right\}u_{l_1 l_2 l_3 \ldots l_N}(y)-\frac{\partial^2 u_{l_1 l_2 l_3 \ldots l_N}}{\partial y^2}(y)\\&=2\beta\sum_{\sigma=1}^{N}\kappa_\sigma\left\{u_{l_1 l_2 l_3 \ldots (l_\sigma-1)\ldots l_N}(y)e^{iK_{\sigma y}y}+u_{l_1 l_2 l_3 \ldots (l_\sigma+1)\ldots l_N}(y)e^{-iK_{\sigma y}y}\right\}\end{aligned} \tag{140}$$

Note that for the case of the simple sinusoidal grating, the transformation

$$u_l(y)=\hat{u}_l(y)e^{i(k_y+lK_y)y} \tag{141}$$

reduces (140) to the more usual form

$$\frac{\partial^2\hat{u}_l(y)}{\partial y^2}+2i(k_y+lK_y)\frac{\partial\hat{u}_l(y)}{\partial y}=\left\{(k_x+lK_x)^2+(k_y+lK_y)^2-\beta^2\right\}\hat{u}_l(y)-2\beta\kappa\left\{\hat{u}_{l-1}(y)+\hat{u}_{l+1}(y)\right\} \tag{142}$$

5.1. Boundary conditions

In the zones in front of and behind the grating where $\kappa_\sigma=0$ equations (140) reduce to the simpler constant index equations:

$$\left\{(k_x+l_1K_{1x}+l_2K_{2x}+\ldots)^2-\beta^2\right\}u_{l_1 l_2 l_3\ldots}(y)-\frac{\partial^2 u_{l_1 l_2 l_3\ldots}}{\partial y^2}(y)=0 \tag{143}$$

These equations define which l modes can propagate in the exterior regions. They have simple solutions of the form

$$u_{l_1 l_2}=Ae^{i\sqrt{\{\beta^2-(k_x+l_1K_{1x}+l_2K_{2x})^2\}}\,y}+Be^{-i\sqrt{\{\beta^2-(k_x+l_1K_{1x}+l_2K_{2x})^2\}}\,y} \tag{144}$$

where the square roots are real for un-damped propagation[6]. Accordingly we may deduce that the form of the front solution comprising the illumination wave and any reflected modes must be of the form

$$u(x,\ y)=e^{ik_x x}e^{i\sqrt{\beta^2-k_x^2}\,y}+\sum_{l_1=-\infty}^{\infty}\sum_{l_2=-\infty}^{\infty}\sum_{l_3=-\infty}^{\infty}\ldots u_{1l_1l_2l_3\ldots}e^{-i\sqrt{\{\beta^2-(k_x+l_1K_{1x}+l_2K_{2x}+\ldots)^2\}}\,y}e^{i(k_x+l_1K_{1x}+l_2K_{2x}+\ldots)x} \tag{145}$$

6 Note that there are modes which propagate inside the grating but which show damped propagation outside.

Likewise the rear solution comprising all transmitted modes must be of the form

$$u(x,\ y)=\sum_{l_1=-\infty}^{\infty}\sum_{l_2=-\infty}^{\infty}\sum_{l_3=-\infty}^{\infty}\ldots u_{3l_1l_2l_3\ldots}e^{i\sqrt{\{\beta^2-(k_x+l_1K_{1x}+l_2K_{2x}+\ldots)^2\}}y}e^{i(k_x+l_1K_{1x}+l_2K_{2x}+\ldots)x} \tag{146}$$

By demanding continuity of the tangential electric field and the tangential magnetic field at the boundaries $y=0$ and $y=d$ we may now use these expressions to define the boundary conditions required for a solution of (135) within the multiplexed grating. At the front surface these are

$$\begin{aligned} i\sqrt{\beta^2-k_x{}^2}(2-u_{000\ldots}(0)) &= \frac{du_{000\ldots}}{dy}\bigg|_{y=0} \\ -i\sqrt{\beta^2-(k_x+l_1K_{1x}+l_2K_{2x}+\ldots)^2}u_{l_1l_2l_3\ldots}(0) &= \frac{du_{l_1l_2l_3\ldots}}{dy}\bigg|_{y=0} \end{aligned} \tag{147}$$

And at the rear surface they take the form

$$i\sqrt{\beta^2-(k_x+l_1K_{1x}+l_2K_{2x}+)^2}u_{l_1l_2l_3\ldots}(d)=\frac{du_{l_1l_2l_3\ldots}}{dy}\bigg|_{y=d} \tag{148}$$

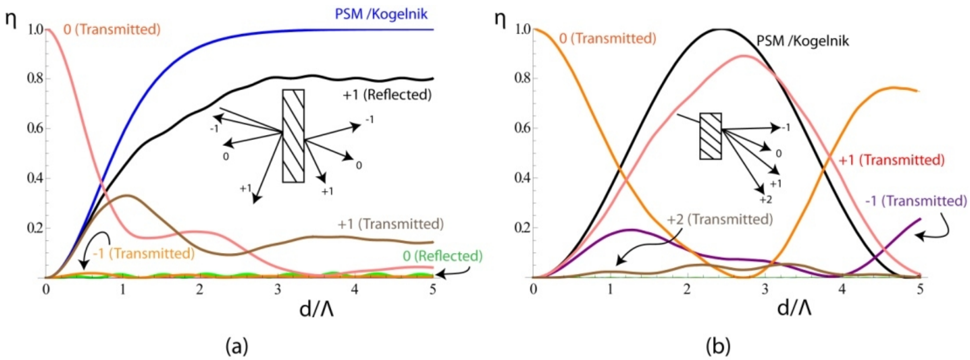

Figure 5. Diffraction Efficiency versus normalised grating thickness according to rigorous coupled wave theory and compared to the PSM and Kogelnik theories at Bragg resonance for (a) the simple reflection grating (n0=1.5, n1/n0=0.331/2, $\theta_c=\theta_r=50^\circ$, $\psi=30^\circ$, $\lambda_c=\lambda_r=532nm$) and (b) the simple transmission grating (n0=1.5, n_1/n_0=0.121/2, $\theta_c=\theta_r=80^\circ$, $\psi=60^\circ$, $\lambda_c=\lambda_r=532nm$).

The modes available for external (undamped) propagation are calculated using the condition

$$\beta^2>(k_x+l_1K_{1x}+l_2K_{2x}+\ldots)^2 \tag{149}$$

http://dx.doi.org/10.5772/53413

Moharam and Gaylord [5] solved the single grating equations (142) using a state-space formulation in which solutions are obtainable through the eigenvalues and eigenvectors of an easily defined coefficient matrix. But one can also solve the more general equations (140), subject to the boundary conditions (147) and (148), using simple Runge-Kutta integration. This is a practical method as long as the number of component gratings within the multiplexed grating is relatively small. Diffraction efficiencies of the various modes are defined as

$$\eta_{l_1 l_2 l_3 \ldots} = \frac{\sqrt{\beta^2 - (k_x + l_1 K_{1x} + l_2 K_{2x} + l_3 K_{3x} + \ldots)^2}}{k_y} u_{l_1 l_2 l_3 \ldots} u_{l_1 l_2 l_3 \ldots}^{*} \qquad (150)$$

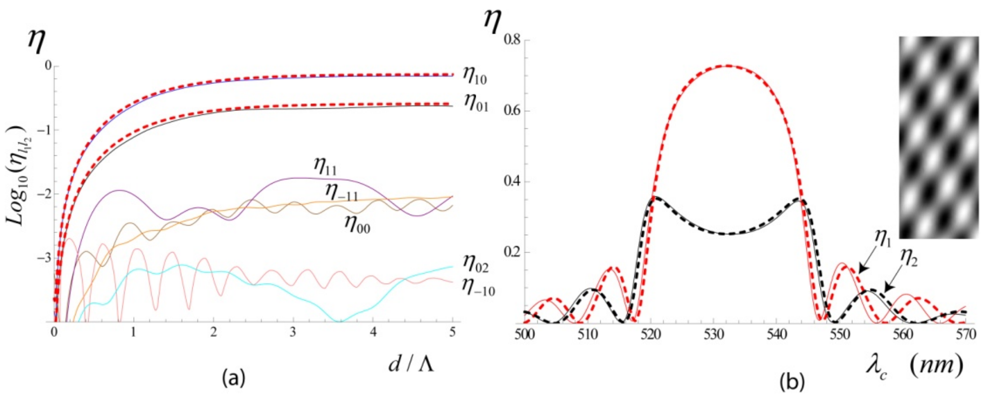

Figure 6. (a) Diffractive Efficiency, η_σ versus normalised grating thickness, d / Λ as predicted by the N-PSM model and by a rigorous coupled wave calculation (RCW) for the case of a twin multiplexed (duplex) reflection grating at Bragg resonance (grating shown in inset photo). The grating is replayed using light of 532nm at an incidence angle of $\Phi_c = 30°$. The grating index modulation of each of the component twin gratings in the duplex has been taken to be $n_1 = 0.2$. The dotted lines indicate the S_1 and S_2 modes of the N-PSM model and the full lines indicate the modes of the RCW calculation. The most prominent RCW modes are the 01 and 10 modes which correspond to the S_1 and S_2modes in N-PSM. The duplex grating has been recorded with a reference beam angle of $\Phi_c = 30°$and with a wavelength of 532nm. One grating in the duplex has a slope of $\psi_1 = 20°$ and the other has a slope of $\psi_2 = -20°$. Note that Λ refers to the larger of the two grating periods. (b) Diffractive Efficiency, η_σ versus replay wavelength, λ_c as predicted by the N-PSM model and by a RCW calculation for the same duplex grating as used in (a) at and away from Bragg resonance. The grating is again illuminated at its recording angle of $\Phi_c = 30°$. A grating index modulation of $n_1 = 0.03$ for each component grating is assumed and a grating thickness of $d = 7\mu m$ is used. The dotted lines indicate the S_1 and S_2 modes of the N-PSM model and the full lines indicate the corresponding 10 and 01 modes of the rigorous coupled wave calculation. In both (a) and (b) the average index inside and outside the grating is $n_0 = 1.5$.

where the fields in this equation are defined either at the front boundary in the case of reflected modes or at the rear boundary in the case of transmitted modes. Note that we are treating the lossless case here and so the sum of all transmitted and reflected efficiencies totals to unity[7].

6. Comparison of PSM and Kogelnik's theory with rigorous CW theory

Equations (140), subject to the boundary conditions (147) and (148) can be solved using either Runge-Kutta integration or through the eigen-method referred to above. This permits the rigorous calculation of the diffraction efficiencies of all modes which are produced by a general grating. Fig.5 shows an example for a simple reflection grating and a simple transmission grating at Bragg Resonance[8]. In the case of the reflection grating a very high index modulation has been assumed. Nevertheless the PSM/Kogelnik estimation is still only 20% out and it is clear that most of the dynamics of the grating is associated with the +1 reflected mode as both PSM and Kogelnik's coupled wave theories assume. In the case of the transmission hologram, a relatively high index modulation is assumed and also a large incidence angle with respect to the grating planes. Here we see again only a small departure from the PSM/Kogelnik estimation but also the presence of the +2 mode.

Fig.6 compares the N-PSM theory with the rigorous equations (140) for the case of a reflection duplex grating formed by the sequential recording of two simple reflection gratings of different slant. The first plot shows the on-Bragg behaviour at high index modulation where evidently good agreement is seen between the two "+1" rigorous modes and the two signal waves in N-PSM despite many other waves being present at much smaller amplitude. The second plot shows the off-Bragg behaviour of the duplex grating at a typical index modulation where excellent agreement is seen between N-PSM and the rigorous calculation.

In general, for the type of index modulations encountered typically in display and optical element holography, the Kogelnik and PSM theories produce fairly accurate estimations of diffractive efficiencies. For multiplexed gratings and for holograms, N-PSM and N-Coupled wave theory similarly produce usefully accurate estimations.

7. Discussion

In this chapter we have presented two analytic methods to describe diffraction in loss-free volume holographic gratings. These are Kogelnik's model and the PSM model. We have shown briefly how the PSM model can be extended to describe spatially multiplexed gratings and holograms. At Bragg resonance the N-PSM model is in exact agreement here with the extension of Kogelnik's model which is known as N-coupled wave theory. Away from Bragg resonance Kogelnik's model and the PSM model give slightly different predictions. But the differences are rather small. This is the same situation when one compares the N-PSM theory with N-coupled wave theory.

We have briefly discussed rigorous coupled wave analysis. Here we have seen that even at high values of index modulation diffraction in the simple reflection grating is controlled

---

7 In the case of the front reflected 000... mode one uses $\eta_{000...} = \frac{\sqrt{\beta^2 - k_x{}^2}}{k_y}(u_{000...} - 1)(u_{000...} - 1)^*$.

8 Note that at Bragg resonance the PSM and Kogelnik models give the same predictions.

http://dx.doi.org/10.5772/53413

predominantly by the "+1" mode. In the simple transmission grating, higher order modes such as the "+2" can become significant if index modulation and incidence angle with respect to the grating planes is high. However the overall conclusion is that for index modulations characteristic of modern display and optical element holography both Kogelnik's coupled wave theory and the PSM model provide a rather good description of diffraction in the volume grating. And this is particularly so in the reflection case where Snell's law conspires to reduce the incidence angles and where RCW analysis shows that the dynamics are controlled really by the "+1" mode alone. RCW analysis also shows that this picture extends to the case of the multiplexed grating - with the implication that it should also apply to holograms.

Finally we should point out that all the theories presented here can be extended to cover more complex cases such as the presence of loss and anisotropy.

Author details

Brotherton-Ratcliffe David

Geola Technologies Ltd, UK

References

[1] H. Kogelnik, “Coupled Wave Theory for Thick Hologram Gratings”, Bell Syst. Tech. J. 48, 2909-47 (1969).

[2] D.J. Cooke and L. Solymar, “Comparison of Two-Wave Geometrical Optics and N-Wave Theories for Volume Phase Holograms”, J.Opt.Soc.Am.70, 1631 (1980).

[3] Brotherton-Ratcliffe, D. “A treatment of the general volume holographic grating as an array of parallel stacked mirrors,” *J. Mod. Optic* 59, 1113–1132 (2012).

[4] X. Ning,“Analysis of multiplexed-reflection holograting s,” J.Opt.Soc.Am. A7, 1436–1440 (1990).

[5] M.G.Moharam and T.K.Gaylord, "Rigorous Coupled Wave Analysis of Planar Grating Diffraction", JOSA, 71, Issue 7, 811-818 (1981).

[6] E.N. Glytis and T.K. Gaylord, "Rigorous 3D Coupled Wave Diffraction Analysis of Multiple Superposed Graings in Ansiotropic Media", Applied Optics, 28, 12, 2401-2421 (1989).

[7] A. B. Bhatia and W. J. Noble, “Diffraction of light by ultrasonic waves,” *Proc. Roy. Soc*. A220, 356-385 (1953).

[8] P. Phariseau, "On the diffraction of light by supersonic waves," *Proc. Ind. Acad. Sci*. 44A 165-170 (1956).

[9] F. Abeles, "Recherches sur la propagation des ondes électromagnétiques sinusoïdales dans les milieux stratifiés. Application aux couches minces," Ann. Phys. (Paris) 5, 596–640 (1950).

[10] R. Jacobsson, "Light reflection from films of continuously varying refractive index," *Progress in Optics*, E. Wolf, ed. North-Holland, Amsterdam, Vol. 5, Chap. 5, pp. 247–286. (1966).

[11] O.S.Heavens,"Optical Properties of Thin Films", Reports on Progress in Physics, XXIII, (1960).

[12] M. P. Rouard, "Etudes des propriétés optiques des lames métalliques très minces," Ann. Phys. (Paris) Ser. II 7, 291–384 (1937).

[13] C.G. Darwin, "The Theory of X-Ray Reflection", Phil.Mag.27, 315-333 (1914).

[14] J.E. Ludman," Approximate bandwidth and diffraction efficiency in thick holograms" Am. J. Phys., 50, 244, (1982).

[15] A. Heifetz, J.T. Shen and M.S. Shariar, "A simple method for Bragg diffraction in volume holographic gratings", Am. J. Phys. 77 No. 7, 623-628 (2009).

[16] R. Guenther, "Modern Optics", John Wiley & sons, ISBN 0-471-60538-7 (1990).

[17] M. G. Moharam and T. K. Gaylord, "Chain-matrix analysis of arbitrary-thickness dielectric reflection gratings," J. Opt. Soc.Am. 72, 187–190 (1982).

[18] D.W. Diehl and N.George, "Analysis of Multitone Holographic Interference Filters by Use of a Sparse Hill Matrix Method," Appl. Opt. 43, 88-96 (2004).

[19] Brotherton-Ratcliffe, D. "Analytical treatment of the polychromatic spatially multiplexed volume holographic Grating," *Appl. Opt*. 51, 7188–7199 (2012).

[20] R. S. Chu and J. A. Kong, "Modal theory of spatially periodic media," IEEE Trans. Microwave Theory Tech. MTT-25,18-24 (1977).